Combined DTI and ASL with T2* imaging Discriminates Between Angiogenic and Highly Diffuse Infiltrative Brain Tumor Models: A Study at 11.7 Tesla

Houshang Amiri[1,2], Anna C. Navis[3], Jolanda de Vries[2], William P. Leenders[3], and Arend Heerschap[1]

[1]*Radiology Department, Radboud University Nijmegen Medical Centre, Nijmegen, Gelderland, Netherlands,* [2]*Tumor Immunology Department, Nijmegen Centre for Molecular Life Sciences, Nijmegen, Gelderland, Netherlands,* [3]*Pathology Department, Radboud University Nijmegen Medical Centre, Nijmegen, Gelderland, Netherlands*

Target audience – Neuro-radiologists, -oncologists, -surgeons, and scientists interested in brain tumor imaging

Purpose – Proper non-invasive differentiation between diffuse infiltrative and angiogenic (parts of) brain tumors may aid in therapy choice and reduce overtreatment. Diffusion tensor imaging (DTI) has been employed to differentiate between these phenotypes in gliomas [1]. However, this is hampered by limited specificity due to inherent heterogeneity of tumor and normal white matter. Thus it is recommended to add other MR approaches. Cerebral blood flow (CBF) and blood oxygenation are expected to differ per phenotype. Therefore we combined DTI with arterial spin-labeling (ASL) and T_2^* imaging to investigate if this could better characterize and discriminate infiltrative from angiogenic tumor tissue. To this aim, we examined genotypic and phenotypic well characterized orthotopic mouse models obtained from human glioma [2].

Methods – We examined 20 athymic Balb/c nude mice bearing orthotopic growing human glioma, including an angiogenic oligodendroglioma (E434, n=6) and two highly invasive astrocytoma models (E468, n=6 ; E473, n=8). When tumor-related symptoms became apparent, imaging was performed. Mice were anesthetized by isoflurane, breathing was monitored and body temperature was maintained at 37.5°C. MRI was performed on an 11.7T BioSpec scanner (Bruker BioSpin, Germany). A circular polarized volume resonator and an actively decoupled mouse brain quadrature surface coil were employed as transmit and receive coils, respectively. Brain anatomy was visualized by a gradient echo (GE) sequence in 3 orthogonal orientations. For DTI experiments, 20 axial slices were acquired with spin-echo echo-planar imaging (SE-EPI). Encoding b-factors of 0s/mm^2 (b0 images; 5×) and 1000s/mm^2 were used and diffusion gradients applied along 30 non-colinear directions (TE=21.4ms, TR=7750ms, Δ=10ms, δ=4ms, number of segments=4, resolution=156×156×500μm^3 and acquisition time (TA)=18min). CBF was obtained by pulsed-ASL with a flow sensitive alternating inversion recovery (FAIR) EPI sequence (TR=18s, TE=12.9ms, FOV=25×25mm^2, slice thickness=1mm, matrix size=128×96, and TA=12min). T_2^* maps were obtained by a multiple GE sequence (TR=1500ms, TE=3.5ms, FA=30°, FOV=25×25mm^2, matrix=256×256, 12 echoes, and TA=5min). All data were analyzed by ParaVision (Bruker Biospin). Circular regions of interest of equal size were selected on T_2-weighted images in the tumor core and in normal appearing brain tissue (NABT) and transferred to the corresponding map. Statistical analyses were performed using Prism (GraphPad Software Inc, CA) by paired (inter-group) and un-paired (intra-group) two-tailed t-test and p values <0.05 were considered significant. Mice were sacrificed following the final MR experiments and brains were formalin fixed and paraffin embedded for further analysis. Tumors were visualized by hematoxylin & eosin (H&E) staining.

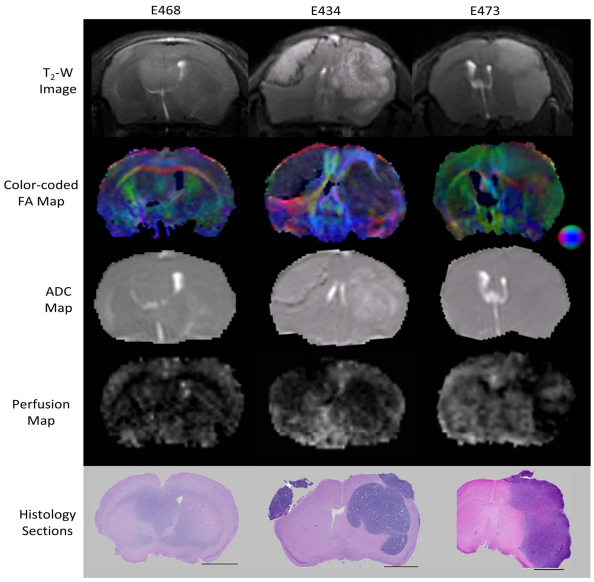

Fig. 1 Representative examples of T_2-weighted images directional color-coded FA, ADC, and perfusion maps as well as histologic sections of the different glioma xenograft models. Scale bars represent 2mm.

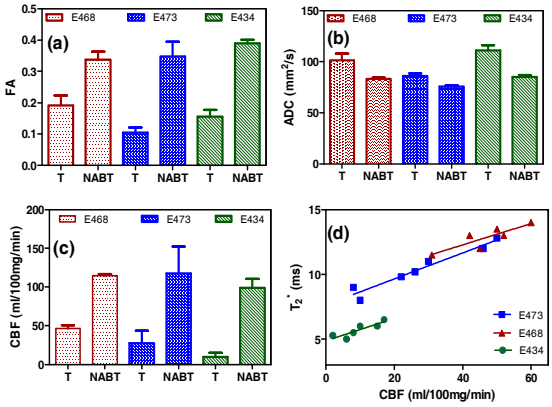

Fig. 2 Statistical analyses of the (a) FA, (b) ADC, (c) CBF and (d) the correlation plot of T_2^* vs CBF for all three study groups.

Results – T_2-weighted images, fractional anisotropy (FA), apparent diffusion coefficient (ADC), and perfusion maps were compared with corresponding histology sections of different xenograft models (Fig 1). Tumor is distinguishable in T_2-weighted images. Color-coded FA maps evidently demonstrate tumor extent in E434 but not in highly diffuse ones. Fibers are destroyed in E434 whereas in E468 tumors do not clearly change the fiber architecture leaving the corpus callosum (CC) intact. Similarly, in E473 fibers are mostly intact although the CC is displaced. Compared to NABT, the FA in tumors decreased significantly (Fig. 2a) for all three models (P<0.01 for E468 and E473 and P<0.001 for E434) and tumor ADC increased (Fig. 2b) substantially (P<0.05 for E468 and P<0.01 for E473 and E434). Among different tumors, E434 did not show a significant change in FA neither with E468 nor with E473 while FA in E468 and E473 tumors was significantly different (P<0.05). Moreover, ADC in E473 significantly differed from other groups (P<0.05 with E468 and P<0.001 with E434) whereas ADCs of E468 and E434 did not differ (P>0.05). Interestingly, all tumors were hypoperfused compared to NABT. Tumor CBF was significantly decreased (Fig. 1c), compared to NABT, in all groups (P<0.001 for all groups). Tumor CBF in both E473 and E434 was decreased once compared with E468, P<0.05 and P<0.001, respectively. Tumor CBF in E473 and E434 also were discriminated (p<0.05). T_2^* significantly decreased in all tumors compared to NABT, which was 18 – 22 ms, with the lowest value for E434. T_2^* correlated with CBF (Fig. 2d).

Discussion – Significant increases in ADC are related to vasogenic edema and decreases in FA to destruction of fiber architecture, which thus are caused by tumor growth. Although the combination of the FA and ADC data mostly differentiated between our models, the E434 and E468 tumors could not be separated in this way. However, by measuring CBF (and T_2^*) it was possible to separate all tumor models. Compared to NABT CBF is decreased in all models, which is thought to be associated with low-grade gliomas [3]. The lowest flow is seen in E434 which likely is attributed to the differences in cellularity and vascularity. Decreases in T_2^* could be a marker for hypoxia because of increased deoxyhemoglobin. Since our models do not present with evident regions of hypoxia, the decrease in T_2^* is likely caused by increased blood volume, which also increases deoxyhemoglobine. Interestingly, CBF correlates positively with T_2^* which is expected because of decreased deoxyhemoglobine with blood flow.

Conclusion – Combined DTI and ASL with T_2^* imaging provides better tumor delineation and phenotypic characterization of angiogenic and diffuse infiltrative tumor tissue.

References – [1] Essig, M., *et al.*, AJNR, 2012. **33**(5): p.803-17. [2] Claes, A., *et al.*, Brain Pathol, 2008. **18**(3): p.423-33. [3] Deibler, A.R., *et al.*, AJNR, 2008. **29**(7): p. 1235-41.